JOURNAL OF SOLID STATE CHEMISTRY 103, 523–527 (1993)

Magnetic and Electric Properties of $La_{1-x}M_xRhO_3$ (M = Ca, Sr, and Ba): Hole Doping in $4d\varepsilon$ Orbitals of Rh^{3+} with Low Spin Configuration

TETSURŌ NAKAMURA, TETSUO SHIMURA, MITSURU ITOH, AND YASUO TAKEDA*

*Research Laboratory of Engineering Materials, Tokyo Institute of Technology, 4259 Nagatsuta-cho, Midori-ku, Yokohama 227, Japan, and *Faculty of Engineering, Mie University, Kamihama-cho, Tsu 514, Japan*

Communicated by J. M. Honig, December 29, 1992

Solid solubility limits of the orthorhombic perovskite systems $La_{1-x}M_xRhO_3$ (M = Ca, Sr, and Ba) are reported to be $x = 0.20$ for M = Ca, $x = 0.10$ for M = Sr, and $x = 0.05$ for M = Ba. The systems are paramagnetic, but show small deviations from the Curie–Weiss law, and are semiconducting, with positive Seebeck coefficients. Both $Rh^{3+}(4d^6)$ and $Rh^{4+}(4d^5)$ are found to be in a low spin state. The dual character of the low-spin Rh^{4+} state with a localized magnetic moment, together with a mobile hole, is demonstrated.

Introduction

The trivalent Rh^{3+} ion with a $4d^6$ configuration is expected to be in the low spin state in the octahedral ligand field of six oxygen ions, and is expected to have no appreciable magnetic moment. All the $ARhO_3$ (A = rare earth elements, In, and Bi) (*1–4*) with perovskite-type structure crystallize in the orthorhombic lattice, with space group *Pbnm* (No. 62). These compounds are semiconducting in the temperature region 78 ~ 450 K (*4*). In the perovskite-type structure, oxygen octahedra share corners with neighboring octahedra, and thereby generate a three dimensional linkage. In this structure electrons and holes in $4d\gamma$ orbitals may become collective. Also, electrons and holes in $4d\varepsilon$ orbitals may become collective when the distances between octahedra are shortened enough to permit overlap of the $4d\varepsilon$ orbitals via O^{2-} p_π orbitals.

We have attempted hole doping into $4d\varepsilon$ orbitals of Rh^{3+} in the low-spin configuration in $LaRhO_3$, by substitution of La^{3+} for Ca^{2+}, Sr^{2+}, and Ba^{2+}. Magnetic susceptibility and electronic resistivity measurements are discussed in conjunction with structural variations.

Experimental

Samples were prepared by a conventional solid state reaction method. Starting compounds were Rh_2O_3 in the high temperature form (*5*), La_2O_3, $SrCO_3$, $CaCO_3$, and $Ba(NO_3)_2$. Their purities were 99.9%, except for La_2O_3, with a purity of 99.99%.

Stoichiometric mixtures of these powders were pulverized, mixed in an agate mortar, and pressed into pellets with a diameter of 12 mm. The pellet was calcined on an alumina boat at 1473 K for 12 hr in flowing O_2 gas, cooled to room temperature, and reground in an agate mortar. The reground powder was compressed again, and sintered at 1523 K for 36–60 hr in flowing O_2 gas.

Quenching from 1523 K to room temperature was required to obtain single-phase

0022-4596/93 $5.00

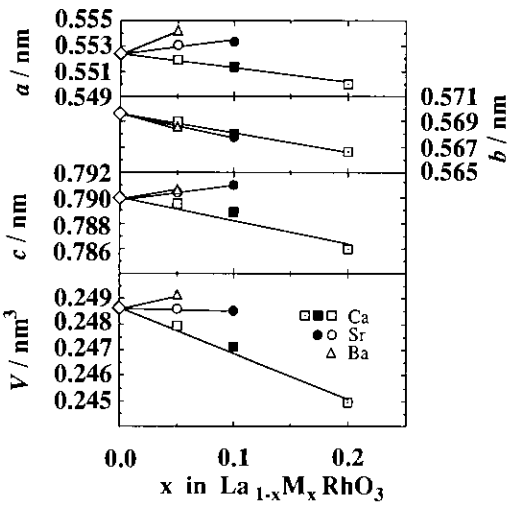

FIG. 1. Lattice constants and cell volume for $La_{1-x}M_xRhO_3$ (M = Ca, Sr, and Ba).

$La_{0.90}Sr_{0.10}RhO_3$, because the substitution limit of La by Sr in $La_{1-x}Sr_xRhO_3$ is close to $x = 0.10$. The phases were identified by powder X-ray diffraction analysis.

The magnetic susceptibility was measured by a SQUID magnetometer from 5 to 300 K. The measured susceptibility $\chi(T)$ value was corrected for orbital diamagnetism of the relevant ions. The resistivity was measured by a dc four probe method from temperature 10 to 300 K.

Results and Discussions

The X-ray diffraction patterns of $La_{1-x}M_xRhO_3$ were rather diffuse, due to a small lattice deformation. The substitution process was confirmed by the disappearance of impurity phases in the diffraction patterns.

Figure 1 shows the lattice constants and cell volumes for $La_{1-x}M_xRhO_3$ (M = Ca, Sr, and Ba). The $LaRhO_3$ space group is orthorhombic *Pbnm* (No. 62) with lattice constants $a = 0.5524(1)$ nm, $b = 0.5697(1)$ nm, and $c = 0.7900(1)$ nm; a and b stretch and shorten, respectively, by Ba and Sr substitution. The length of c increases with Ba or Sr substitution, and satisfies the relation $a < c/\sqrt{2} < b$. The cell volume increases by Ba substitution and decreases slightly with Sr substitution. These results reflect the ionic size difference between Ba^{2+} and Sr^{2+}; the radii of Ba^{2+}, Sr^{2+}, and La^{3+} are 0.161, 0.144, and 0.136 nm (*6*), respectively. No extra peaks occur in the diffraction patterns of all substituted samples which do not also exist in the diffraction pattern for $LaRhO_3$. Thus, no change of space group seems to occur by substitution. Since the radii of Rh^{4+} and Rh^{3+} are 0.060 and 0.067 nm (*6*), respectively, the decrease of cell volume by Sr substitution may be attributed to the formation of Rh^{4+} with a small ionic radius. In the Ca substitution the length of three axes and the cell volume decrease.

Table I shows the degree of orthorhombicity $(b - a)/(b + a)$ of $La_{1-x}M_xRhO_3$; here r_A is the average ionic radius of the A-site (La-site) ion. With the ionic radii of Ca^{2+} and of La^{3+} at the 12-coordination site 0.1360 and 0.1340 nm (*6*), respectively, the orthorhombicity becomes small as the ionic radius of the substituting ion increases.

The limit of substitution is 10% for Sr, 20% for Ca, and 5% for Ba. Beyond these limits, impurity phases such as SrO, Rh_2O_3, CaO, and $BaRhO_3$ (*7*) appear in the diffraction pattern. High pressure oxygen treatment at high temperature was attempted to extend the solubility limit of $La_{1-x}Sr_xRhO_3$. However, RhO_2 was detected as an impurity

TABLE I

ORTHORHOMBICITY OF $La_{1-x}M_xRhO_3$ (M = Ca, Sr, AND Ba)

Samples $ARhO_3$	Average ionic radius of A site r_A/nm	Orthorhombicity $(b - a)/(b + a)$
$LaRhO_3$	0.1360	1.530×10^{-2}
$La_{0.95}Ca_{0.05}RhO_3$	0.1359	1.529×10^{-2}
$La_{0.90}Ca_{0.10}RhO_3$	0.1358	1.484×10^{-2}
$La_{0.80}Ca_{0.20}RhO_3$	0.1356	1.487×10^{-2}
$La_{0.95}Sr_{0.05}RhO_3$	0.1364	1.375×10^{-2}
$La_{0.90}Sr_{0.10}RhO_3$	0.1368	1.291×10^{-2}
$La_{0.95}Ba_{0.05}RhO_3$	0.1372	1.282×10^{-2}

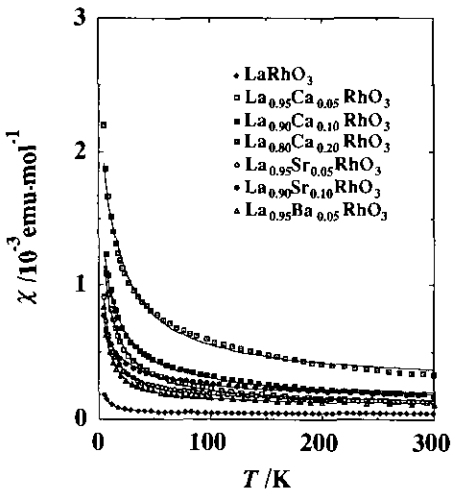

FIG. 2. Temperature dependency of the magnetic susceptibility for $La_{1-x}M_xRhO_3$ (M = Ca, Sr, and Ba). The lines express the calculated susceptibility for $La_{0.80}Ca_{0.20}RhO_3$ using the data for χ_0, C, and Θ in Fig. 3.

phase in the high pressure oxygen treated samples, and the degree of crystallinity was not improved.

Figure 2 shows the temperature dependence of the magnetic susceptibility for $La_{1-x}M_xRhO_3$. Even though the susceptibility of $LaRhO_3$ was not quite zero, it is certain that Rh^{3+} in $LaRhO_3$ takes up the low-spin configuration. The very small value of susceptibility for $LaRhO_3$ may be ascribed to the localized magnetic moments of free Rh^{4+} or Rh^{2+} ions, due to a small degree of oxygen nonstoichiometry.

The susceptibilities for $LaRhO_3$ exactly follows the Curie–Weiss (CW) law $\chi = \chi_0 + C/(T - \Theta)$ between 5 and 300 K. The susceptibility of substituted samples also seems to follow the CW law between 5 and 300 K; the estimated values of the temperature-independent term χ_0, the Curie constant C, and the Curie–Weiss temperature Θ obtained through a least squares fit are shown in Fig. 3. For the substituted samples, this fit is not as good as for $LaRhO_3$. The curves in Fig. 2 represent calculated magnetic susceptibility for $La_{1-x}M_xRhO_3$ using the fitting data shown in Fig. 3. Obviously, the experimental susceptibility does not strictly follow the CW law.

While the magnetic susceptibility for substituted samples differs somewhat from the CW law, the $La_{1-x}M_xRhO_3$ system seems to be paramagnetic. The fact that no hysteresis in susceptibility with changes of magnetic field was observed in any samples at 5 K supports this hypothesis.

Deviations from the CW law can be ascribed to random mixing of the localized Rh^{4+}-state among the octahedral Rh^{3+} sites, which introduces a heterogeneous magnetic interaction and a local distribution of the Curie–Weiss constant C. The values of χ_0, C, and Θ in Fig. 3 for the substituted samples are interpreted in terms of the paramagnetism of delocalized carriers, the magnitude of the localized moment, and the strength of the magnetic interaction between localized moments, respectively.

The temperature-independent term χ_0 in Fig. 3 increases with increasing amounts of substitution, but does not vary significantly among the dopants. If χ_0 is mainly due to Pauli paramagnetism of mobile carriers, χ_0 depends only on the carrier density. In this sense, the lattice distortion or its relaxation,

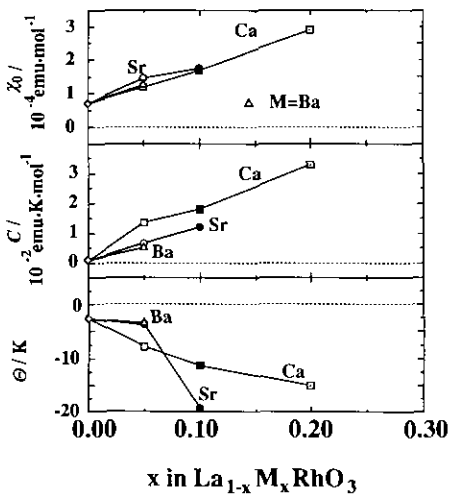

FIG. 3. Change in χ_0, C, and Θ by substitution for $La_{1-x}M_xRhO_3$ (M = Ca, Sr, and Ba).

documented in Table I, does not influence the carrier density.

The Curie constant C increases almost linearly increasing substitution. The rate of this increase is somewhat higher for M = Ca than for M = Sr or Ba. The experimental values of C for $La_{0.90}Sr_{0.10}RhO_3$ and $La_{0.90}Ca_{0.10}RhO_3$, for example, are 0.0122 and 0.0179 emu · K · mole^{-1}, respectively, which are closer to the theoretical value C_L = 0.0375 emu · K · mole^{-1} based on the low spin Rh^{4+} and Rh^{3+} states, rather than the spin-only values based on the high spin Rh^{4+} and low spin Rh^{3+} (C_H = 0.4375 emu · K · mole^{-1}), or the intermediate spin Rh^{4+} and low spin Rh^{3+} (C_M = 0.1875 emu · K · mole^{-1}). This tendency holds also for the other composition $x \neq 0.10$ in $La_{1-x}M_xRhO_3$. Therefore, it is reasonable to conclude that Rh^{4+} is in the low spin state.

Negative Curie–Weiss temperatures for all the samples in Fig. 3 indicate an antiferromagnetic interaction between localized moments, but no antiferromagnetic transition was observed. A rapid decrease in Curie–Weiss temperatures Θ for $La_{0.90}Sr_{0.10}RhO_3$ might result from an increase in the 180° antiferromagnetic superexchange interactions (*8*), the increased Rh–O–Rh overlaps being caused by the relaxation of lattice distortions documented in Table I.

Figure 4 shows the variation of the logarithm of the resistivity of $La_{1-x}M_xRhO_3$ as a function of temperature. It is obvious that $LaRhO_3$ exhibits semiconducting behavior. Through substitution the resistivity decreases, but its temperature coefficient is still negative from 5 K to 300 K. In a qualitative measurement the Seebeck coefficient was found to be positive; this indicates that the carriers are holes in $4d\varepsilon$ orbitals.

The resistivity at 300 K decreases with increasing substitution of each element. This reduction of resistivity is strongest for Sr^{2+} substitution, and for Ca^{2+} substituted samples is almost equal to that in Ba^{2+} substituted samples. This trend in resistivity,

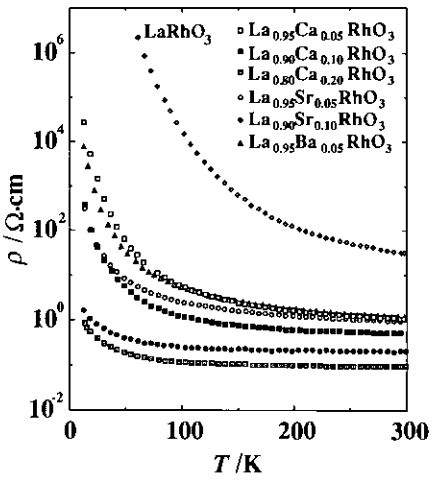

FIG. 4. Temperature dependency of resistivity for $La_{1-x}M_xRhO_3$ (M = Ca, Sr, and Ba).

$\rho = 1/n\mu e$, cannot be accounted for by a difference in carrier density n_h (hole density), since there is no real difference in χ_0, that is in n_h, for the different substitutions shown in Fig. 3. Thus, the tendency can only be explained by a difference in carrier mobility $\mu_h \propto \tau/m_h$, which is associated with the bandwidth and is quite sensitive to the lattice deformations. As shown in Table I, the orthorhombicity is obviously smaller in $La_{1-x}Sr_xRhO_3$ than in $La_{1-x}Ca_xRhO_3$. It is reasonable to assume that the overlap among Rh $4d\varepsilon$ orbitals and O $2p\pi$ orbitals increases when the lattice distortion decreases. This larger overlapping of orbitals leads to smaller resistivities in Sr-substituted samples. The ionic radius of Ba^{2+} may so large that overlap of $4d\varepsilon$ orbitals and $p\pi$ orbitals is not improved when the orthorhombic distortion decreases by substitution. A similar explanation was given by one of the authors (*9*) for the metallic resistivities of polycrystalline $AMoO_3$ (A = Ba, Sr, and Ca); $\rho(SrMoO_3) < \rho(CaMoO_3) < \rho(BaMoO_3)$.

The tendency of the resistivity to increase with decreasing temperature, especially for Ca-substituted samples in Fig. 4, is attributed to the domination of carrier localization

via lattice deformation against an orbital overlap via volume contraction.

In summary, we have succeeded in doping some mobile holes into the $4d\varepsilon$ orbitals of Rh^{3+} ($4d^6$) states in the perovskite solid-solution systems $La_{1-x}M_xRhO_3$ (M = Ca, Sr, and Ba).

Acknowledgments

Part of this work was supported by a Grant-in-Aid for Scientific Research from the Ministry of Education, Science, and Culture. The treatment of samples at high temperature under high oxygen pressure was carried out by Professor Gérard Demazeau of Bordeaux University.

References

1. A. Wold, B. Post, and E. Banks, *J. Am. Chem. Soc.* **79,** 6365 (1957).
2. A. Wold, R. J. Arnott, and W. J. Croft, *Inorg. Chem.* **2,** 972 (1963).
3. I. S. Shaplygin, I. I. Prosychev, and V. B. Lazarev, *Russ. J. Inorg. Chem.* **31,** 1649 (1986).
4. R. D. Shannon, *Acta. Crystallogr. Sect. B* **26,** 447 (1970).
5. H. Levia, R. Kershaw, K. Dwight, and A. Wold, *Mater. Res. Bull.* **17,** 1539 (1982).
6. R. D. Shannon, *Acta. Crystallogr. Sect. A.* **32,** 751 (1976).
7. B. L. Chamberland and J. B. Goodenough, *J. Solid State Chem.* **39,** 114 (1981).
8. E. E. Havinga, *Philips Res. Rep.* **21,** 432 (1966).
9. S. Hayashi, R. Aoki, and T. Nakamura, *Mater. Res. Bull.* **14,** 409 (1979).